

## Electronic transitions in single-walled carbon nanotubes: A resonance Raman study

P. M. Rafailov,\* H. Jantoljak, and C. Thomsen

*Institut für Festkörperphysik, Technische Universität Berlin, Hardenbergstrasse 36, D-10623 Berlin, Germany*

(Received 23 August 1999; revised manuscript received 21 December 1999)

Resonance excitation profiles of the high-frequency peaks in the Raman spectra of single-walled carbon nanotubes normalized to the scattering intensity of  $\text{CaF}_2$  are presented. We find separate resonances of metallic and semiconducting tubes throughout the visible and the near-IR excitation range. The resonance shift of samples with different mean diameters confirm the inverse proportionality of the resonant transition energy to the tube diameter. Smaller diameter tubes are found to have sharper resonances than larger tubes due to a  $1/d^2$  dependence of the Raman cross section.

### I. INTRODUCTION

Resonance Raman spectroscopy has affirmed itself as a powerful method for studying electronic transitions in semiconductors. Recently it has been applied to the investigation of the vibrational and electronic properties of carbon nanotubes. The sensitivity of the Raman cross section to the nanotube band structure is enhanced by the electronic one-dimensional (1D) quantum confinement as  $k$  vectors can take continuous values only in axial direction.<sup>1,2</sup> The resonant scattering processes originate from the corresponding 1D singularities in the electronic density of states with an energy gap, which is inversely proportional to the diameter and depends on the tube symmetry.<sup>3,4</sup> The diameter dependence of the scattering intensity was established experimentally through comparative Raman measurements on graphite, multiwalled and single-walled nanotubes.<sup>5</sup>

There are two main vibrational bands in the Raman spectrum of a carbon nanotube: a low-energy mode at  $150\text{--}200\text{ cm}^{-1}$ , which arises from a radial breathinglike vibration with a strong van der Waals intertube contribution,<sup>6,7</sup> and a high-energy mode (HEM) at  $\approx 1600\text{ cm}^{-1}$  with a displacement pattern derived from the  $E_{2g}$  bond-stretching mode of graphite. The relative intensity of the individual HEM peaks changes dramatically<sup>8-10</sup> when varying the excitation energy in the range  $1.5\text{ eV} \leq \hbar\omega_l \leq 2.2\text{ eV}$  compared to energies outside this range. The main peaks broaden and strong lines appear on the low-energy side of the HEM band. This behavior was attributed to a resonant enhancement of metallic nanotubes in the samples over semiconducting tubes.<sup>4,9,10</sup> In an attempt to determine the excitation profile of this resonance Pimenta *et al.*<sup>11</sup> recently normalized their spectra to the intensity of the HEM peak at  $1592\text{ cm}^{-1}$ , a procedure valid only in the absence of an excitation-energy dependence of this peak in semiconducting nanotubes. However, as we show in this contribution, the  $1592\text{-cm}^{-1}$  peak is resonant at energies corresponding to transitions in semiconducting tubes. We determine experimentally these energies by measuring the scattering efficiencies normalized to a reference material ( $\text{CaF}_2$ ) with a known Raman efficiency. In addition, we confirm the predicted inverse diameter dependence of the allowed electronic transitions for both semiconducting and metallic tubes. Our measurements provide an opportunity to determine the tight-binding parameter  $\gamma_0$  (nearest-neighbor electronic overlap integral) for two differ-

ent mean-diameter tubes from the resonance profiles in the Raman spectra.

### II. EXPERIMENT

The carbon nanotubes used in the present study were produced by the arc-discharge method. A mixture of metallic catalysts (Ni and Y) and graphite provided the growth of high-density single-walled nanotubes (SWNT), which are organized in ropes with a triangular lattice structure.<sup>12</sup> For the investigation of diameter-dependent electronic effects we selected two samples with different mean values of the tube diameter. From transmission electron microscopy (TEM) images the majority of SWNT diameters  $d$  was found to be  $1.1\text{--}1.5\text{ nm}$  and  $1.2\text{--}1.7\text{ nm}$  in the two samples, following a Gaussian-like distribution with mean values  $d_0 = 1.3\text{ nm}$  and  $1.45\text{ nm}$  and a halfwidth of about  $0.1\text{ nm}$ .

Recent nanodiffraction measurements<sup>13</sup> showed that ropes of SWNT prepared under the same conditions as ours consist of tubes of uniform diameter but different chiral angles, in agreement with the scanning tunneling microscopy (STM) results.<sup>14</sup> Since tube chirality within a given tube category (metallic or semiconducting) does not have a strong influence on the electronic density of states we neglect effects of chirality in what follows.<sup>3</sup>

The Raman spectra were recorded on a Dilor XY 800 spectrometer equipped with a liquid-nitrogen-cooled charge-coupled device (CCD). An  $\text{Ar}^+/\text{Kr}^+$ -ion gas laser and a Titan sapphire laser were used for excitation energies between  $1.59$  and  $2.55\text{ eV}$  and an excitation intensity below  $500\text{ W/cm}^2$ . The measurements were performed at room temperature in backscattering geometry. Each spectrum was recorded after carefully maximizing the scattering intensity and calibrated by the Raman intensity of the optical mode of  $\text{CaF}_2$  recorded under the same experimental conditions. We fitted our Raman spectra with three peaks, implying that each peak actually corresponds to an envelope over a series of lines arising from different nanotubes with slightly differing frequencies. The optical properties of  $\text{CaF}_2$  are constant over the examined energy range ( $1.59\text{--}2.55\text{ eV}$ );<sup>15</sup> a necessary correction to determine the resonant excitation profiles is to account for the varying optical penetration depth of the nanotube sample  $\delta(\omega_{l(s)})$  for the incident (scattered) light that determines the scattering volume. From optical measurements<sup>4</sup> we found  $\delta(\omega_l)$  to decrease approximately

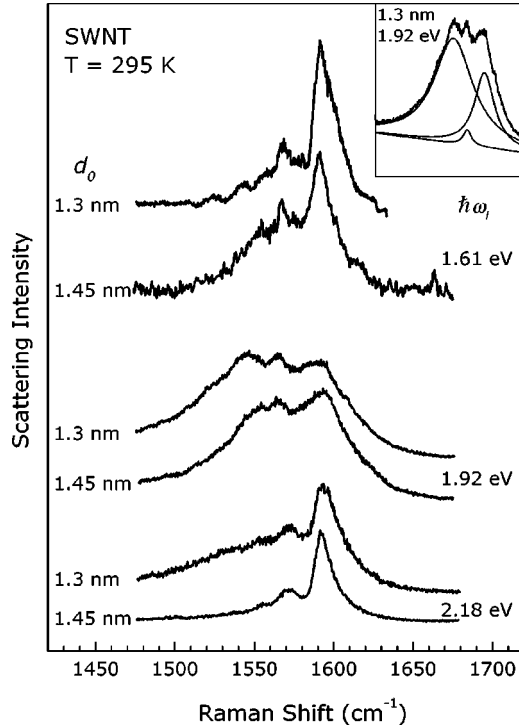


FIG. 1. Raman spectra of the high-energy mode of the two examined samples at three different excitation energies. Inset: A fit of the high-energy mode with three peaks.

by a factor of 2 with  $\delta(\omega_l) \approx \delta(\omega_s)$  when varying the excitation energy from 1.6 to 2.6 eV. This normalization was performed for the two peaks at  $1550 \text{ cm}^{-1}$  and  $1592 \text{ cm}^{-1}$ , the former being characteristic of metallic tubes, the latter of semiconducting tubes.

### III. RESULTS AND DISCUSSION

Raman spectra of the high-energy modes in both samples at three different excitation energies are shown in Fig. 1. For excitation energies above the metallic resonance the Raman spectra of the two samples look similar as they do below the metallic resonance (two lowest and uppermost traces in Fig. 1). The strongest peak at these excitation energies is at  $1592 \text{ cm}^{-1}$  in both samples, while the one at  $1571 \text{ cm}^{-1}$  (1.45-nm sample) is shifted slightly to higher frequencies in the 1.3-nm sample (curves with  $\hbar\omega_l = 2.18 \text{ eV}$ ). At an excitation energy of 1.92 eV we find the metallic resonance; for the smaller mean-diameter tubes the metallic peak at  $1550 \text{ cm}^{-1}$  is enhanced more than that for the larger one. Within the metallic resonance the phonon modes of the 1.3-nm sample are at lower frequencies compared to the 1.4-nm sample. This is best seen for the  $1550 \text{ cm}^{-1}$  mode, which is at  $1546 \text{ cm}^{-1}$  and  $1551 \text{ cm}^{-1}$  for the smaller- and larger-diameter SWNT samples, respectively. This frequency shift was explained by Kasuya *et al.* as a result of different mean diameters in the zone-folding approximation.<sup>5</sup> We fitted the HEM band with three peaks as shown in the inset of Fig. 1; the normalized integrated intensities of the  $1592$ - and  $1550$ - $\text{cm}^{-1}$  peaks for all excitation energies are summarized in Fig. 2.

The resonance energies  $E_{ii}$  of a particular SWNT are determined by transitions  $v_i \rightarrow c_i$  from a singularity in the  $i$ th

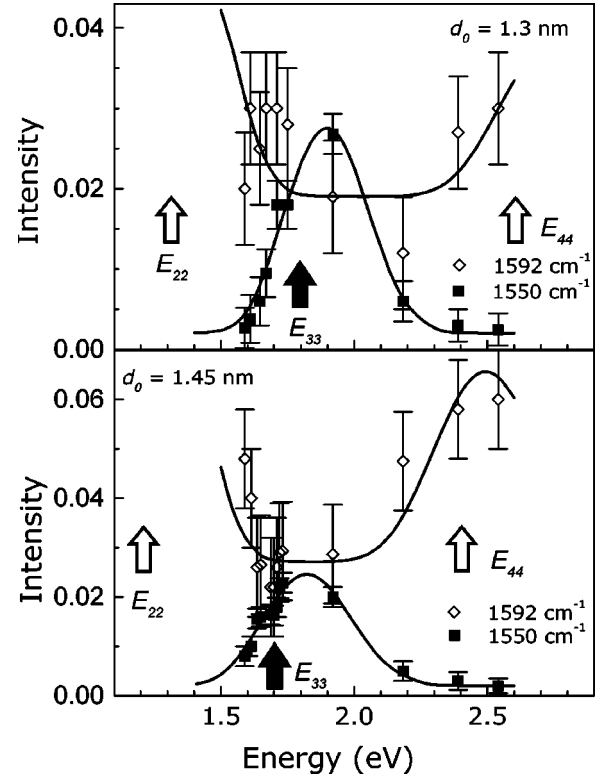


FIG. 2. Resonant excitation profiles of the Raman peaks arising from metallic and semiconducting tubes for  $d_0 = 1.3 \text{ nm}$  (upper panel) and  $d_0 = 1.45 \text{ nm}$  (lower panel). The solid (open) points represent the intensity ratio of the peak at  $1550 \text{ cm}^{-1}$  ( $1592 \text{ cm}^{-1}$ ) to that of the  $\text{CaF}_2$  phonon, and the solid lines are fits to these experimental data using Eq. (4). For the fit of the  $1592\text{-cm}^{-1}$  peak intensity we added a constant. The arrows indicate the  $E_{ii}$  as given by the best-fit  $\gamma_0$  value.

valence band to a singularity in the  $i$ th conduction band.<sup>16</sup> The transitions  $v_i \rightarrow c_j$  with  $i \neq j$  occur with a much smaller probability for symmetry reasons,<sup>16</sup> and are neglected in the following treatment. Typical semiconducting SWNT's have three pairs of such singularities within  $\pm 1.5 \text{ eV}$  of the Fermi level<sup>17</sup> separated by about  $0.5$ – $0.7 \text{ eV}$ . Metallic nanotubes exhibit only one pair of spikes in this energy range with a gap of  $1.5$ – $2.2 \text{ eV}$  accounting for the metallic resonance. These transitions were confirmed by combined scanning tunneling microscopy and spectroscopy (STM and STS).<sup>14,18</sup> In particular, the separation of the first pair of singularities for metallic SWNT's with diameters  $1.2$ – $1.4 \text{ nm}$  was found to be  $1.7$ – $2.0 \text{ eV}$ .

For a particular nanotube the transition energies  $E_{ii}$  not too far from the Fermi level may be expressed as  $E_{ii} = 2ia_0\gamma_0/d$  for semiconducting ( $i = 1, 2, 4, 5, \dots$ ) and metallic ( $i = 3, 6, \dots$ ) tubes.<sup>3</sup> Here  $a_0 = 0.142 \text{ nm}$  is the nearest-neighbor distance of the C atoms and  $\gamma_0$  the nearest-neighbor electronic overlap integral. The  $\gamma_0$  values reported range from  $2.5 \text{ eV}$  as used in *ab initio* calculations<sup>19</sup> to  $3.14 \text{ eV}$  as obtained for 3D graphite.<sup>2</sup> STM experiments<sup>18</sup> yield  $2.7 \text{ eV}$  and resonance Raman experiments<sup>11</sup>  $2.95 \text{ eV}$ . A typical diameter distribution will result in quasicontinua of electronic transitions for both semiconducting and metallic SWNT's.

We calculate the resonance Raman profile by considering the matrix element  $K(\hbar\omega_l)$  of the Raman process according

TABLE I. Values of the electronic overlap integral  $\gamma_0$  and the damping constant  $\gamma$  as obtained from fits to the resonance excitation profiles of two SWNT samples with different mean diameters  $d_0$ . The corresponding electronic transition energies are listed as well.

$d_0$ (nm)	Freq. (cm <sup>-1</sup> )	$\gamma_0$ (eV)	$\hbar\gamma$ (eV)	$E_{22}$ (eV)	$E_{33}$ (eV)	$E_{44}$ (eV)	Type
1.3	1546	2.73	0.03		1.8		Metallic
1.3	1592	3.0	0.033	1.3		2.6	Semiconducting
1.45	1551	2.9	0.033		1.7		Metallic
1.45	1592	3.05	0.037	1.2		2.4	Semiconducting

to Ref. 20:

$$K(\hbar\omega_l) = \frac{1}{\hbar^2} \sum_{ij} \frac{M_i H_{ij} M_j}{(\omega_l - \omega_i - i\gamma_i)(\omega_s - \omega_j - i\gamma_j)}, \quad (1)$$

where  $\omega_{l,s}$  are the frequencies of the incident (scattered) light,  $\omega_{i,j}$  are the frequencies of the resonant electronic transitions with matrix elements  $M_{i,j}$ ,  $\gamma_i$  is the damping factor of the  $i$ th transition,  $H_{ij}$  is the electron-phonon Hamiltonian matrix element, and the summation is over all possible direct transitions, which we may convert into an integral over the joint density of states. The universal expression for the joint density of states of nanotubes of Mintmire and White<sup>19</sup> has an explicit inverse proportionality to diameter. For every  $E \geq E_{ii}$  there is a contribution  $\rho_i(E) = a_0 E/d \gamma_0 \sqrt{E^2 - E_{ii}^2}$ , the quantum confinement becoming enhanced for smaller-diameter tubes. As the phonon energy is large compared to the width of the peaks in the electronic density of states, we consider incoming and outgoing resonances according to

$$K(\hbar\omega_l) = M \frac{1}{\hbar} \int \frac{\rho(\hbar\omega) d\omega}{(\omega_l - \omega - i\gamma)(\omega_l - \omega_{ph} - \omega - i\gamma)}, \quad (2)$$

where  $\hbar\omega_{ph}$  is a phonon energy, and where we have assumed, as is usually done, that the matrix elements are constant and the damping factor is the same for both transitions. In order to keep the problem tractable, we approximate the square-root singularities by a  $\delta$  function and obtain for each transition  $v_i \rightarrow c_i$

$$K_i(\hbar\omega_l) = \frac{a_0 E_c M}{d \gamma_0 (\hbar\omega_l - E_{ii} - i\hbar\gamma) (\hbar\omega_l - \hbar\omega_{ph} - E_{ii} - i\hbar\gamma)}, \quad (3)$$

where  $E_c \gg E_{ii}$  is a cutoff energy and  $\hbar\omega_{ph} = 0.199$  eV and 0.194 eV in the semiconducting and metallic tubes, respectively.

The Raman intensity of a particular nanotube due to the electronic transitions  $E_{ii}$  is proportional to the absolute square of the matrix element, and we average over the Gaussian-like distribution of diameters in our sample to obtain the contribution of each transition to the Raman signal. The index  $i$  labels again the transitions in semiconducting ( $i = 1, 2, 4, 5, \dots$ ) and metallic ( $i = 3, 6, \dots$ ) tubes:

$$I_i(\hbar\omega_l) = \sum_d \frac{1}{d^2} \frac{A \exp\{-\frac{1}{2}[(d-d_0)/\sigma]^2\}}{[(E_{ii} - \hbar\omega_l)^2 + \hbar^2\gamma^2][(E_{ii} - \hbar\omega_l + \hbar\omega_{ph})^2 + \hbar^2\gamma^2]}, \quad (4)$$

where  $A$  is a normalization factor. Equation (4) differs from that used by Pimenta *et al.*<sup>11</sup> in the weighting factor  $d^{-2}$ , which comes from the the universal joint density of states. Our expression thus properly accounts for the stronger resonant enhancement of tubes with smaller diameter.

Figure 2 displays the experimental results together with the calculated resonance profile where we summed Eq. (4) over diameters within  $\pm 2\sigma$  of  $d_0$  and, for the semiconducting tubes, over the index  $i$ . The diameter enters Eq. (4) explicitly and through the diameter dependence of the transition energies  $E_{ii}$ . We find the metallic resonance with a maximum at  $\approx 1.9$  and 1.8 eV for the 1.3- and 1.45-nm diameter sample, respectively. The  $\gamma_0$  values from the fit differ somewhat;  $\gamma_0 = 2.73$  eV and  $\gamma_0 = 2.9$  eV for the two diameters. The corresponding transition energies of the mean-diameter tube are  $E_{33} = 6a_0\gamma_0/d_0 = 1.80$  eV and 1.70 eV and indicated as solid arrows in Fig. 2. The apparent shift between the maxima and the transition energy  $E_{ii}$  of the mean-

diameter tube is a direct consequence of the  $1/d^2$  enhancement of the Raman signal by smaller-diameter tubes [Eq. (4)]. The semiconducting resonance maxima are outside our excitation range;  $E_{ii}$  as determined from the best-fit values of  $\gamma_0$  are  $E_{22} = 1.3$  eV and  $E_{44} = 2.6$  eV ( $d_0 = 1.3$  nm) and  $E_{22} = 1.2$  eV and  $E_{44} = 2.4$  eV ( $d_0 = 1.45$  nm) (open arrows in Fig. 2). The rising edges of the fit describe our data well. The broadening parameter determined from our fit is  $\hbar\gamma = 30$  meV and somewhat larger than that previously reported [20 meV (Refs. 11 and 21)]. The results are summarized in Table I.

#### IV. CONCLUSIONS

Three main conclusions follow from our normalized resonant Raman spectra of semiconducting and metallic SWNT's: (1) We identify the resonances  $E_{22}$  and  $E_{44}$  of semiconducting nanotubes in addition to  $E_{33}$  in metallic tubes, rendering it improper to internally normalize the me-

tallic nanotube by the semiconducting nanotube peaks, which suggests sharper resonances than actually present. (2) The experimentally determined semiconducting and metallic resonance energies show an inverse-diameter dependence, as expected theoretically. (3) In accordance with the  $1/d^2$  resonance enhancement [Eq. (4)] the smaller-tube resonance is stronger and sharper than that of the larger tube, and  $E_{ii}$  is at lower energies than the maxima in the resonance profiles.

## ACKNOWLEDGMENTS

We thank P. Bernier and C. Journet for providing us with the nanotube samples. We gratefully acknowledge a careful reading of the manuscript by S. Reich and valuable discussions with A. R. Goñi. P.M.R. acknowledges financial support from the Deutscher Akademischer Austauschdienst—Germany.

\*Permanent address: Faculty of Physics, University of Sofia, BG-1164 Sofia, Bulgaria.

<sup>1</sup>A.M. Rao, E. Richter, S. Bandow, B. Chase, P.C. Eklund, K.A. Williams, S. Fang, K.R. Subbaswamy, M. Menon, A. Thess, R.E. Smalley, G. Dresselhaus, and M.S. Dresselhaus, *Science* **275**, 187 (1997).

<sup>2</sup>M.S. Dresselhaus, G. Dresselhaus, and P.C. Eklund, *Science of Fullerenes and Carbon Nanotubes* (Academic Press, New York, 1996).

<sup>3</sup>J.C. Charlier and Ph. Lambin, *Phys. Rev. B* **57**, R15 037 (1998).

<sup>4</sup>H. Kataura, Y. Kumazawa, Y. Maniwa, I. Umezū, S. Suzuki, Y. Ohtsuka, and Y. Achiba, *Synth. Met.* **103**, 2506 (1999).

<sup>5</sup>A. Kasuya, Y. Sasaki, Y. Saito, K. Tohji, and Y. Nishina, *Phys. Rev. Lett.* **78**, 4434 (1997).

<sup>6</sup>U.D. Venkateswaran, A.M. Rao, E. Richter, M. Menon, A. Rinzler, R.E. Smalley, and P.C. Eklund, *Phys. Rev. B* **59**, 10 928 (1999).

<sup>7</sup>C. Thomsen, S. Reich, A.R. Goñi, H. Jantoljak, P.M. Rafailov, I. Loa, K. Syassen, C. Journet, and P. Bernier, *Phys. Status Solidi B* **215**, 435 (1999).

<sup>8</sup>M. Sugano, A. Kasuya, K. Tohji, Y. Saito, and Y. Nishina, *Chem. Phys. Lett.* **292**, 575 (1998).

<sup>9</sup>A. Kasuya, M. Sugano, and C. Horie, *Phys. Rev. B* **57**, 4999 (1998).

<sup>10</sup>M.A. Pimenta, A. Marucci, S.D.M. Brown, M.J. Matthews, A.M. Rao, P.C. Eklund, R.E. Smalley, G. Dresselhaus, and M.S.

Dresselhaus, *J. Mater. Res.* **13**, 2396 (1998).

<sup>11</sup>M.A. Pimenta, A. Marucci, S.A. Empedocles, M.G. Bawendi, E.B. Hanlon, A.M. Rao, P.C. Eklund, R.E. Smalley, G. Dresselhaus, and M.S. Dresselhaus, *Phys. Rev. B* **58**, R16 016 (1998).

<sup>12</sup>C. Journet, W.K. Maser, P. Bernier, A. Loiseau, M. Lamy de la Chapelle, S. Lefrant, P. Deniard, R. Lee, and J.E. Fischer, *Nature (London)* **388**, 756 (1997); C. Journet and P. Bernier, *Appl. Phys. A: Mater. Sci. Process.* **67**, 1 (1998).

<sup>13</sup>L. Henrard, A. Loiseau, C. Journet, and P. Bernier, *Synth. Met.* **103**, 2533 (1999).

<sup>14</sup>T.W. Odom, J.L. Huang, P. Kim, and C.M. Lieber, *Nature (London)* **391**, 62 (1998).

<sup>15</sup>*Physical Quantities*, edited by I. S. Grigoriev and E. Z. Meilikhov (Energoatomizdat, Moscow, 1991).

<sup>16</sup>E. Richter and K.R. Subbaswamy, *Phys. Rev. Lett.* **79**, 2738 (1997).

<sup>17</sup>R. Saito, T. Takeya, T. Kamura, G. Dresselhaus, and M.S. Dresselhaus, *Phys. Rev. B* **57**, 4145 (1998).

<sup>18</sup>J.W.G. Wildöer, L.C. Venema, A.G. Rinzler, R.E. Smalley, and C. Dekker, *Nature (London)* **391**, 59 (1998).

<sup>19</sup>J.W. Mintmire and C.T. White, *Phys. Rev. Lett.* **81**, 2506 (1998).

<sup>20</sup>R.M. Martin and L.M. Falikov, in *Light Scattering in Solids I*, edited by M. Cardona, Topics of Applied Physics Vol. 8 (Springer, New York, 1983).

<sup>21</sup>The definition of the broadening parameter used by Pimenta *et al.* differs from ours by a factor of  $2\hbar$ .